Coherent Atomic Soliton Molecules

Chenyun Yin,[1] Natalia G. Berloff,[1] Víctor M. Pérez-García,[2] Valeryi A. Brazhnyi,[3] and Humberto Michinel[4]

[1]*Department of Applied Mathematics and Theoretical Physics, University of Cambridge, Cambridge, CB3 0WA, United Kingdom.*
[2]*Departamento de Matemáticas, E. T. S. I. Industriales, Universidad de Castilla-La Mancha 13071 Ciudad Real, Spain.*
[3]*Centro de Física do Porto, Faculdade de Ciências, Universidade do Porto, R. Campo Alegre 687, Porto 4169-007, Portugal*
[4]*Área de Óptica, Facultade de Ciencias, Universidade de Vigo, As Lagoas s/n, Ourense, E-32004 Spain.*

We discuss the dynamics of interacting atomic bright solitons and dark bubbles in bulk immiscible Bose-Einstein condensates. Coherent matter-wave clusters can be constructed using dark-bright pairs with appropriate phases. In two dimensions we describe novel types of matter-wave molecules without a scalar counterpart that can be seen as bound states of vector objects.

PACS numbers: 05.45.Yv, 03.75.Lm

Introduction.- One of the most remarkable achievements in quantum physics in the last decade was the experimental realization of coherent atomic matter waves with Bose-Einstein condensates (BECs) of ultra-cold alkaline atoms [1]. Because of the inter-atomic interactions, BECs support different types of quantum nonlinear coherent excitations: dark [2], bright [3] and gap atomic solitons [4], vortices, vortex rings and related structures [5], shock waves [6], different types of vector solitons [7], and others [8]. Many other nonlinear phenomena have been theoretically studied in BECs [9].

A challenging open problem both in BEC experiments and in nonlinear science at large is the construction of complex molecule-like coherent matter-wave structures. A possible strategy, that we explore in this letter, is to use atomic solitons and bubbles as bricks to construct stable matter wave aggregates which display phase-dependent properties. Related problems have been considered in nonlinear optics in relation with the propagation of optical beams in media with saturable nonlinearities [10], it being very difficult to construct even metastable long-living soliton clusters. Nonlocal interactions allow for the creation of soliton clusters but local interactions such as those present in ordinary BECs pose great difficulties [11]

In the field of matter-waves, trains with a finite number of quasi-one dimensional bright solitons have been observed to be robust and stable [3] due to the presence of the trap [12]. However, the idea does not work for higher dimensions due to the blow-up phenomenon [3]. With repulsive nonlinearities, dark solitons always repel each other and cannot form bound states [13].

In this letter we will show how multicomponent homonuclear Bose-Einstein condensates in the immiscible regime allow for the construction of robust solitonic molecules. These matter-wave clusters display phase-dependent properties due to their coherent nature.

Physical system.- We will consider two-component homonuclear BECs with atoms in two different hyperfine states $|1\rangle$ and $|2\rangle$ [14]. We will work in the immiscible regime and consider droplets of atoms in component $|2\rangle$ to be phase separated from a component $|1\rangle$ assumed to have a much larger number of particles.

1-D atomic soliton molecules.- BECs tightly confined along two transverse directions are quasi-one dimensional and ruled in the mean field limit by the equations [15, 16]

$$i\frac{\partial u_j}{\partial t} = -\frac{1}{2}\frac{\partial^2 u_j}{\partial x^2} + \left(\sum_{k=1,2} g_{jk}|u_k|^2 - \mu + \Delta_j\right) u_j, \quad (1)$$

for $j = 1, 2$. Without loss of generality we will take the adimensional chemical potential $\mu = 1$, and $\Delta_1 = 0$. Immiscibility implies that $g_{12}^2 > g_{11}g_{22}$. The normalization for u_2 is given by $\int_{\mathbb{R}} |u_2|^2 = 2(a_{22}/a_0)N_2$, a_{22} and N_2 being the s-wave scattering length and number of atoms in $|2\rangle$. Finally $a_0 = \sqrt{\hbar/m\omega_\perp}$ is the length-scale in which the adimensional spatial units are measured. Since we are interested on the bulk dynamics as in ring-shaped condensates no longitudinal traps will be considered.

Let us first study the case of equal interaction coefficients, $g_{ij} = 1, i, j = 1, 2$, that is very close to the realistic situation e.g. in Rb [14] or Na [17]. The phenomena to be described in this paper are not dependent on this specific choice of parameters and indeed, later we will consider the effect of tunning interactions [18]. In the former case, Eqs. (1) have explicit dark-bright soliton solutions

$$u_1 = i\sqrt{\mu}\sin\alpha + \sqrt{\mu}\cos\alpha\tanh\left(\kappa\left[x - q(t)\right]\right), \quad (2a)$$

$$u_2 = \sqrt{\frac{N_B\kappa}{2}}e^{i\phi}e^{i\Omega t}e^{i\kappa x\tan\alpha}\mathrm{sech}\left(\kappa\left[x - q(t)\right]\right). \quad (2b)$$

where $\kappa = \sqrt{\mu\cos^2\alpha + (N_B/4)^2} - N_B/4$ is the inverse of the wave packet length, $\Omega = \kappa^2(1 - \tan^2\alpha) - \Delta_2$, and the soliton center position is $q(t) = X_0 + t\kappa\sin\alpha$ [15].

The repulsive nature of the interaction between dark solitons prevents the formation of bound states of dark solitons. Concerning bright solitons, their mutual forces in the absence of external effects depend on the phase differences, $\Delta\phi = |\phi_1 - \phi_2|$, going from repulsive for $\Delta\phi = 0$

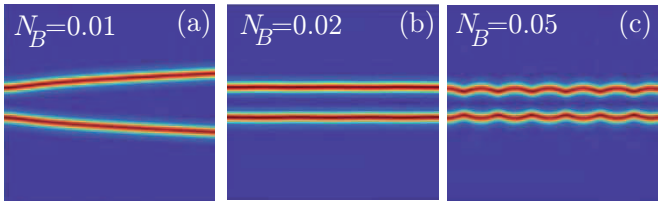

FIG. 1: Interaction of two vector dark-bright solitons (1,2) for different amplitudes of the bright component $N_{B,1} = N_{B,2}$ (a) 0.01 (b) 0.02 (c) 0.05. Other parameter values are given in the text. We plot pseudocolor plots of $|u_2(x,t)|^2$ ("bright" component) on the range $x \in [-20, 20], t \in [0, 2000]$.

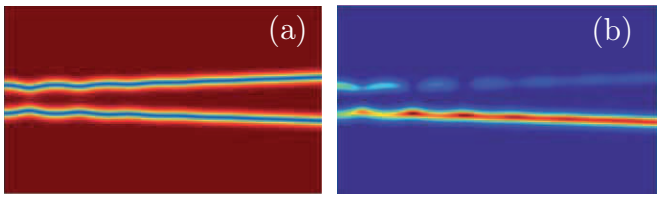

FIG. 2: Interaction of two vector dark-bright solitons for $N_B = 0.05$ and $\Delta\phi = 3$. Other parameters as in Fig. 1. Shown are pseudocolor plots of (a) $|u_1(x,t)|^2$ and (b) $|u_2(x,t)|^2$ on the range $x \in [-20, 20], t \in [0, 2000]$.

to attractive for $\Delta\phi = \pi$. There is a critical intermediate regime for $\Delta\phi$ in which unstable bound states can be constructed.

Thus, a vector object including a dark soliton in one component and a bright soliton in another component could lead to a stable bound state with a second vector soliton of the same type when the coherent interactions between the dark and the "droplet-like" bright component have opposite directions leading to what can be considered as a coherent molecule.

We have studied numerically the interaction between two (hereafter denoted 1 and 2) initially static ($\alpha_1 = \alpha_2 = 0$) vector solitons given by Eqs. (2). Other parameters are $\mu = 1$, $\Delta_2 = 0$ and the initial positions are $X_{0,1} = 3$, $X_{0,2} = -3$. In order to have attractive interactions between the bright components we choose $\Delta\phi = \pi$. Our results are summarized in Fig. 1.

Small droplets of atoms of the second species are not

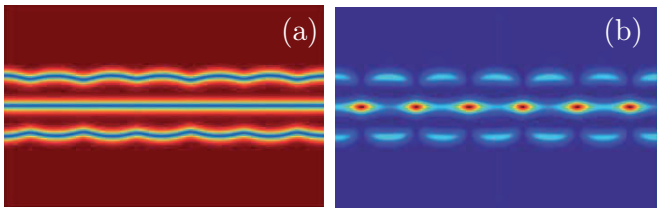

FIG. 3: Interaction of three vector dark-bright solitons for $N_B = 0.05$, $X_{0,1} = -6$, $X_{0,2} = 0$, $X_{0,3} = 6$. Other parameters as in Fig. 1. Shown are pseudocolor plots of (a) $|u_1(x,t)|^2$ and (b) $|u_2(x,t)|^2$ on the range $x \in [-20, 20], t \in [0, 2000]$.

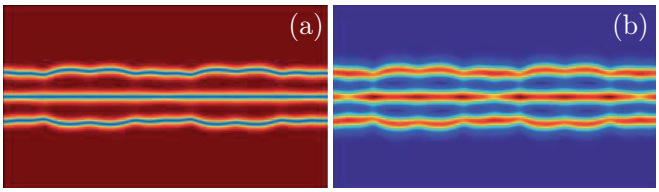

FIG. 4: Interaction of three vector dark-bright solitons for $N_B = 1$, $X_{0,1} = -8$, $X_{0,2} = 0$, $X_{0,3} = 8$ with $\phi_1 = 0$, $\phi_2 = 2.28$, $\phi_3 = 0$. Other parameters as in Fig. 1. Shown are pseudocolor plots of (a) $|u_1(x,t)|$ and (b) $|u_2(x,t)|$ on the range $x \in [-30, 30], t \in [0, 1000]$.

able to stop the outgoing motion induced by the repulsive interaction between the black solitons in $|1\rangle$. However, for larger numbers of atoms in $|2\rangle$ we obtain a bound state of the two vector solitons, with a threshold number of atoms of about $N_B = 0.18$. This is a remarkable result leading to a bound *pair of dark-bright solitons in a system where all the interactions are repulsive* due to the effective attraction provided by the phase between the "droplets" of atoms in component $|2\rangle$.

The formation of these bound states is sensitive to the specific phase difference between the bright droplets in $|2\rangle$ as it is seen in Fig. 2, where a change of the phase difference from π to 3 suffices to destabilize the system.

However, the addition of more components leads to a very interesting feature: although the atoms in $|2\rangle$ feature a less trivial dynamics, they are still able to sustain the multisoliton bound state provided the beating period is faster than the typical evolution times of the dark component. An example is shown in Fig. 3.

Curiously, multisoliton states are much more robust to perturbations in the phase differences (see Fig. 4). We have also constructed atomic soliton molecules with more than three atoms, e.g. five soliton bound states, etc.

Two-dimensional molecules.- When passing to higher dimensions the phenomenology changes essentially due to the fact that the more natural building blocks are vortices for the first component hosting a "droplet" of the second component. In the scalar case, moving two-dimensional bound states were found in Ref. [19] and correspond to vortex pairs of opposite circulation and rarefaction pulses. A similar phenomenology arises in the two-component case in the miscible regime [20]. As the velocity increases, the distance between vortices of opposite circulation decreases to zero. The solutions at even higher velocity are localized density perturbations without zeros of the wavefunction. In two dimensions the sequence of solutions terminates with solutions approaching zero energy and momentum as the velocity U approaches the speed of sound.

Due to the structure of the vortex velocity field it is not possible to use the interactions of the bright part to construct bound states of equally charged vortices. Thus, unless a simple extension of the previous ideas is

not possible we will see in what follows that a novel phenomenology arises very different from the classical one described in Ref. [19] that can be linked to the presence of bound states of solitary wave structures.

In what follows we will systematically construct solitary waves moving with speed U along the $x-$direction in two-dimensional two-component condensates in the phase-separation regime as solutions of the coupled GP system (1), where $\partial/\partial t \to -U\partial/\partial x$, and $\partial^2/\partial x^2 \to \nabla^2$

$$iU\frac{\partial \psi_1}{\partial x} = \frac{1}{2}\nabla^2\psi_1 + \left(1 - |\psi_1|^2 - \alpha|\psi_2|^2\right)\psi_1, \quad (3a)$$

$$iU\frac{\partial \psi_2}{\partial x} = \frac{1}{2}\nabla^2\psi_2 + \left(\Lambda - \alpha|\psi_1|^2 - |\psi_2|^2\right)\psi_2 \quad (3b)$$

together with the boundary conditions $|\psi_1| \to 1, \psi_2 \to 0$, as $|\mathbf{x}| \to \infty$. In the phase separation regime $\alpha = g_{12}/g_{11} = g_{12}/g_{22} > 1$. Here $\Lambda = \mu_2/\mu_1$ where μ_1 and μ_2 are the dimensional chemical potentials of ψ_1 and ψ_2. We solve numerically the discretized version of Eqs. (3) by a Newton-Raphson algorithm combined with a secant algorithm to find Λ for a given constraint on $N_2 = \int |\psi_2|^2\, dx\, dy$. We obtain a family of solutions characterized by the velocity of propagation U, energy, E and impulse $\mathbf{p} = (p_1 + p_2, 0)$, given by

$$E = \int \left[\frac{1}{2}|\nabla\psi_1|^2 + \frac{1}{2}|\nabla\psi_2|^2 + \alpha|\psi_1|^2|\psi_2|^2 \right. \quad (4a)$$

$$\left. + \frac{1}{2}(1 - |\psi_1|^2)^2 + \frac{1}{2}|\psi_2|^4 - \Lambda|\psi_2|^2\right] dxdy, \quad (4b)$$

$$p_1 = \mathrm{Im}\left[\int_{\mathbb{R}^2} (\psi_1^* - 1)\frac{\partial \psi_1}{\partial x}\right] dxdy, \quad (4c)$$

$$p_2 = \mathrm{Im}\left[\int_{\mathbb{R}^2} \psi_2^*\frac{\partial \psi_2}{\partial x} dxdy\right]. \quad (4d)$$

The resulting families of solutions are given on Fig. 5 for various choices of N_2 together with the Jones-Roberts (JR) dispersion relations [19] for one-component condensates. For a given speed U, solitary solutions with higher α have lower energy and higher impulse. Firstly, in contrast with the JR solutions, there is a stationary solitary wave corresponding to the ground state of the system with all the mass of the second component forming a radially symmetric "bubble" in the centre of the depleted first component. This complex has a nonzero energy E_{gs}. As the velocity increases from zero, the bubble becomes oblate in the direction of the motion with the velocity field of the first component is that of a dipole as Fig. 6 illustrates. There is a point on the dispersion curve where the velocity reaches its maximum – the inflection point. As energy and momentum continue to increase, the velocity decreases and the solutions become pairs of vortices of opposite circulation in the first component with the second component condensing in the vortex cores. In general the bubble-like solutions, for small E can be seen as a bound state of a JR rarefaction pulse and a mobile "filling" of the second component. Fig. 5(b) shows

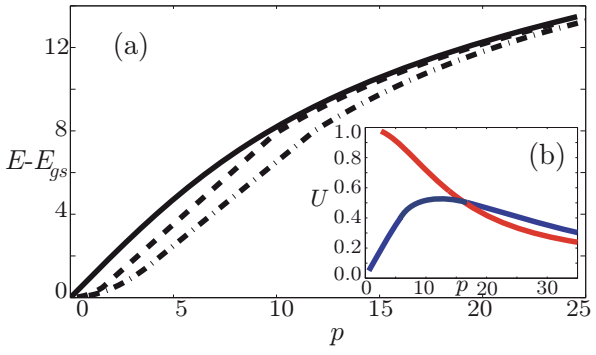

FIG. 5: (Color online) (a) Energy $(E - E_{gs})-$ impulse $(p = p_1 + p_2)$ dispersion curve of the solitary wave solutions of Eqs. (3) for $\alpha = 1.2$ and various choices of N_2. The upper solid line corresponds to $N_2 = 0$, i.e. the JR dispersion curve, shown here for comparison. To ease comparison we subtract the ground state energy E_{gs} in the plot. Dashed black line corresponds to $N_2 = 8$ and the dash-dot line corresponds to $N_2 = 20$. (b) Velocity as a function of momentum for $N_2 = 20$, the red curve corresponding to the JR case. The solid line corresponds to the JR case.

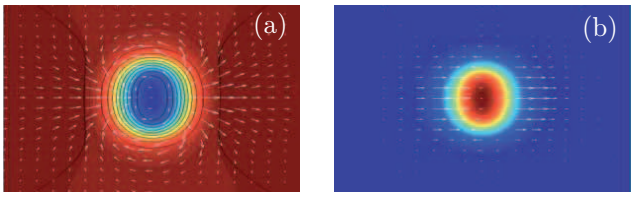

FIG. 6: (Color online) A stationary bound state solution for $U = 0.2$, $N_2 = 80$. (a) $|\psi_1(x,y)|^2$ (b) $|\psi_2(x,y)|^2$. Shown are pseudocolor plots of the densities, arrows indicating the direction of the local current density $\boldsymbol{j} = -\mathrm{Re}\,(i\psi\nabla\psi^*)$ and for (a) a few contour lines (black solid lines). The spatial region shown in the plot is $(x,y) \in [-30,30] \times [-20,20]$

that there is a maximum velocity for the propagation of these solutions well separated from the sound speed velocity what can be physically interpreted as a signature of the mass of the second component, the heavier being the second component the smaller being this maximum velocity. To study the collisional properties of these localized structures we have simulated the evolution of two bubbles set on a colliding course. Initially the bubbles are separated by a large distance, so that individually they are accurately represented by the solutions we found. We have observed several possible outcomes of such collisions summarized in Fig. 7. Almost identical slow colliding bubbles may form a bound stationary state even when they collide with an offset. Bubbles moving with large velocities may scatter at $\pi/2$ angle resembling the collision of two pairs of vortices of opposite circulation. Almost elastic collisions between these structures were observed when the velocities or masses of the bubbles were very different. We have observed that a bound state is more likely to be formed when bubbles have similar phases of

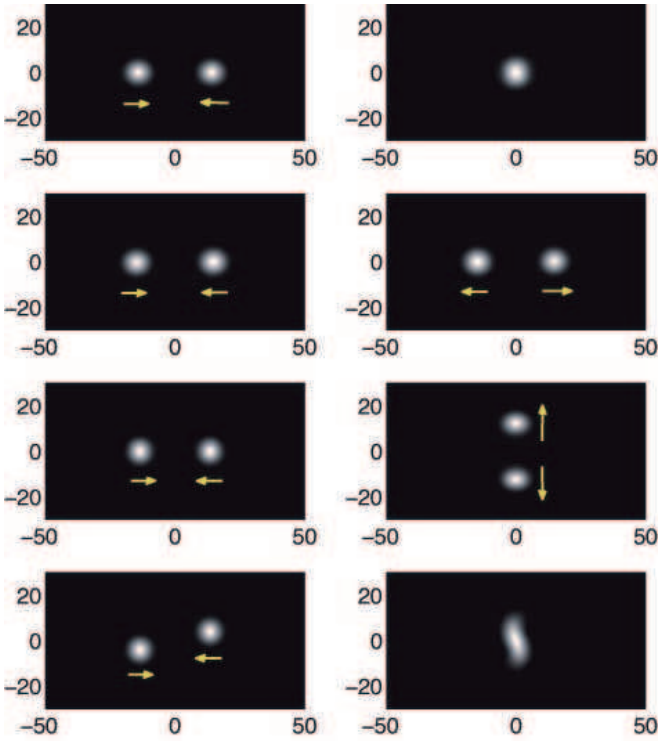

FIG. 7: Outcomes of coherent bubble-droplet pairs collisions. Density snapshots of the second component are shown before (left column) and after (right column) the collision. In the first row, identical incident bubbles with $U = 0.1, N_2 = 40, p = 6.36, E = 2.99$ form a bound state. In the second row, for $U_1 = U_2 = 0.2$ incident bubbles with the same speed but different sizes emulate a elastic collision (left bubble: $N_2 = 40, E = 5.6, p = 14.9$, right bubble: $N_2 = 50, E = 7.7, p = 20.1$). In the third row, identical bubbles (parameters being $U = 0.2, N_2 = 40, E = 5.6, p = 14.9$) emulate vortex recombination. In the fourth row, identical bubbles (same as those in third row) collide with an offset of 8 dimensionless units and form a bound state.

the second component and move slowly. In all such collisions, a small fraction of the total mass is lost and carried away by sound waves. The outgoing bubbles are solitary wave solutions as verified by energy-impulse calculations.

Conclusions.- We have discussed the dynamics of interacting bubble-droplet pairs in immiscible Bose-Einstein condensates. Coherent atomic soliton molecules made up of dark-bright soliton pairs with appropriate phases can be constructed in 1D scenarios. In two-dimensions, we have found novel types of robust bubble-like solitons without a scalar counterpart that can be seen as a bound state of two vector objects. Our ideas can be used to construct coherent atomic molecules made up of solitons.

Acknowledgements.- This work has been supported by grants FIS2007-29090-E (Ministerio de Ciencia e Innovación, Spain), PGIDIT04TIC383001PR (Xunta de Galicia) and PCI-08-0093 (Junta de Comunidades de Castilla-La Mancha, Spain). NGB acknowledges support from EPSRC-UK and Isaac Newton Trust. VAB acknowledges support from the FCT grant, PTDC/FIS/64647/2006. We want to acknowledge David Novoa (U. Vigo) for discussions.

[1] L. Pitaevskii, S. Stringari, *Bose-Einstein condensation*, Oxford University Press, Oxford (2003).
[2] S. Burger *et al.*, Phys. Rev. Lett. **83**, 5198 (1999); S. Stellmer *et al.*, *ibid.*, **101**, 120406 (2008); A. Weller, *et al.*, *ibid.*, **101**, 130401 (2008).
[3] K. E. Strecker, *et al.*, Nature **417**, 150 (2002); L. Khaykovich et al., Science **296**, 1290 (2002); S. L. Cornish, S. T. Thompson, and C. E. Wieman, Phys. Rev. Lett. **96**, 170401 (2006).
[4] B. Eiermann *et al.*, Phys. Rev. Lett. **92**, 230401 (2004).
[5] M.R. Matthews, *et al.*, Phys. Rev. Lett. **83**, 2498 (1999); J.R. Abo-Shaeer, *et al.*, Science **292**, 476 (2001); B. P. Anderson *et al.*, Phys. Rev. Lett. **86** 2926 (2001).
[6] Z. Dutton *et al.*, Science, **293**, 663 (2001); J.J. Chang, P. Engels, M. A. Hoefer, Phys. Rev. Lett. **101**, 170404 (2008); M. A. Hoefer, *et al.*, Physica D **238**, 1311 (2009); R. Meppelink, *et al.*, Phys. Rev. A **80**, 043606 (2009).
[7] N.S. Ginsberg, J. Brand and L.V. Hau, Phys. Rev. Lett. **94**, 040403 (2005); C. Becker *et al.*, Nature Phys. **4**, 496 (2008).
[8] P. Engels, C. Atherton, and M. A. Hoefer, Phys. Rev. Lett. **98**, 095301 (2007); I. Shomroni, *et al.*, Nature Phys. **5**, 193 (2009).
[9] R. Carretero-González, D. J. Frantzeskakis and P. G. Kevrekidis, Nonlinearity **21** R139 (2008); V. M. Pérez-García, *et al.*, Physica D **238**, 1289 (2009).
[10] M. Soljacić, S. Sears and M. Segev, Phys. Rev. Lett. **81**, 4851 (1998); E. A. Ostrovskaya, *et al.*, Opt. Lett. **24**, 327 (1999); J. J. García-Ripoll *et al.*, Phys. Rev. Lett. **85**, 82 (2000); A.S. Desyatnikov and Y. S. Kivshar, Phys. Rev. Lett. **87**, 033901 (2001); A. S. Desyatnikov *et al.*, Opt. Lett. **26**, 435 (2001); Y.V. Kartashov, *et al.*, J. Opt. Soc. Am. B **19**, 2682 (2002); L.-C. Crasovan *et al.*, Phys. Rev. E, **67**, 046610 (2003).
[11] F. Maucher, *et al.*, arXiv:0911.5020v1; D. Buccoliero, *et al.*, Physica B: Condensed Matter, **94**, 351 (2007).
[12] V. S. Gerdjikov, B. B. Baizakov, M. Salerno, N. A. Kostov, Phys. Rev. E **73**, 046606 (2006).
[13] W. Zhao and E. Bourkoff, Opt. Lett.**14**, 1371 (1989).
[14] C. J. Myatt, *et al.*, Phys. Rev. Lett. **78**, 586 (1997); M. R. Matthews *et al.*, Phys. Rev. Lett. **81** 243 (1998).
[15] Th. Busch, J. R. Anglin, Phys. Rev. Lett. **87**, 010401 (2001).
[16] V. M. Pérez-García, H. Michinel, and H. Herrero, Phys. Rev. A **57**, 3837 (1998).
[17] D. Stamper-Kurn, *et al.*, Phys. Rev. Lett. **80**, 2027 (1998).
[18] G. Thalhammer, *et al.*, Phys. Rev. Lett. **100**, 210402 (2008); S. B. Papp, J. M. Pino, C. E. Wieman, Phys. Rev. Lett. **101**, 040402 (2008).
[19] C.A. Jones and P.H. Roberts, J. Phys. A **15** 2599 (1982); C.A.Jones, S.J. Putterman, and P.H. Roberts, J. Phys. A: Math. Gen. **19** 2991 (1986).
[20] N. G. Berloff, Phys. Rev. Lett. **94**, 120401 (2005).